

# **Experimental and analytical study of novel rapid freeze casting technique to fabricate 3D-shaped gelatin nanofibers**

Ali Zamanian<sup>1</sup>, Farnaz Ghorbani<sup>1,2\*</sup>, Neda Arabi<sup>1</sup>

<sup>1</sup>Biomaterials Research Group, Nanotechnology and Advanced Materials Department, Materials and Energy Research Center, Karaj, Iran.

<sup>2</sup>Department of Biomedical Engineering, Science and Research Branch, Islamic Azad University, Tehran, Iran.

\*Corresponding author: Department of Biomedical Engineering, Science and Research Branch, Islamic Azad University, Tehran, Iran, E-mail: farnaz\_ghorbani.1991@yahoo.com

Received: 10 June 2018, Accepted: 25 June 2018

---

## **Abstract**

Nanofibrous scaffolds are often used to reconstruct damaged tissues/organs. Unfortunately, the lack of producing three-dimensional (3D) nanofiber results in their restricted applications. Therefore, bulky-shaped gelatin nanofibers were fabricated through novel rapid freeze casting (RFC) technique to simulate extracellular matrix (ECM) and accelerate the regeneration. Formation of 3D-shaped fibers in the range of 200-1000 nm with approximately 98% porosity and significantly improved mechanical stability compared with conventional freeze casting (CFC) technique is one of the strengths of this study even though both RFC and CFC macrostructures are similar. Outcomes proved this novel technique reduced hydrophilicity and controlled biodegradation rate owing to applying a high freezing gradient in order to the production of thin pores. The viability of more than 90% cells compared with control group confirmed the biocompatibility of constructs and supporting cellular proliferation. In brief, novel RFC gelatin nanofibers represented original physicochemical and mechanical features for further in-vitro and in-vivo studies.

**Keyword:** Fiber Technology; Rapid Freeze Casting (RFC); Scaffold; Tissue engineering; Polymers.

---

## **1. Introduction**

The primary goal of tissue engineering is an expansion of the healing process through replacing injured tissues by injecting cells to defect sites, simulating extracellular matrix (ECM) and delivering biomolecules (1). Currently, biomimetic scaffolds have

attracted numbers of scientists owing to providing a substrate for cellular proliferation, preventing deformation of the defect site and feasibility of tapping biomolecules (2). The nanofibrous scaffolds gain popularity among a variety of

fabrication techniques due to the high surface area to volume ratio, the possibility of using a broad range of materials, facility of functionalization, cost-effectively and user-friendly (3). There are some techniques to produce nanofibers such as electrospinning (4), phase separation (5), self-assembly (6), melt fibrillation (7), island-in-sea (8) and gas jet (9). All the prepared fibers by these techniques have some disadvantages leads to introducing and developing novel fibers via rapid freeze casting (RFC) method. The restriction over industrial productivity, low yield, time-consuming process and above all lack of production of the 3D nanofibers (macroscopic view) in other techniques result in rising RFC to compensate all the defects. Herein, RFC technology introduced as a novel approach for the fabrication of nanofibrous scaffolds with 3D macrostructure to simulate natural ECM. Also, the capability of fibers to supply physicochemical and mechanical requirements has been studied. Obtained results create a substrate for further investigations.

## 2. Materials and methods

Gelatin (Mw= 40-50 kDa), Glutaraldehyde (25%,  $d= 1.058 \text{ gr/cm}^3$ ), NaOH (Mw= 39.997 gr/mol), and Ethanol (Mw= 46.07 gr/mol) were purchased from Merck Co. Ltd.

(Germany). Phosphate Buffered Saline (PBS, Powder, pH= 7.4) was purchased from Aprin Advanced Technologies Development Co. Ltd. (Iran). Sodium borohydride ( $\text{NaBH}_4$ , Mw= 37.83 gr/mol), Thiazolyl Blue Tetrazolium Bromide (MTT, Mw= 414.32 gr/mol), Dimethyl Sulfoxide (DMSO, 1X), and L-Glutamine (Mw= 146.14 gr/mol) were purchased from Sigma Co. Ltd. (USA). Dulbecco's Modified Eagle's Medium (DMEM) was purchased from Mehregan Biotechnology Co. Ltd. (Iran). Fetal bovine serum (FBS) and penicillin-streptomycin were purchased from Gibco-BRL, Life Technologies Co. Ltd. (NY). All chemicals were used directly without further purification. Aqueous solutions were prepared with double distilled water. Homogeneous gelatin solutions with a concentration of 1 % (w/v) were prepared in deionized water at 40 °C for more than 12 hours stirring. Then, before freezing operation, the polymeric solution was cross-linked by glutaraldehyde (0.5 wt.%) as explained in Table. 1. Freezing operation was followed by using the home-made setup as described in previous study (10). So, the solution was transferred to polytetrafluoroethylene (PTFE) mold. The mold is connected to liquid nitrogen tank via a copper rod.

**Table 1: Synthesizing condition for various gelatin scaffolds**

Codes	Concentration (%w/v)	Glutaraldehyde (%w/w)	Freezing Rate (°C/min)
R1	1	0.5	1
R3	1	0.5	3
R6	1	0.5	6

The connected heater to this rod controls the temperature gradient. Solutions were frozen at the constant direction and temperature gradients of 1, 3 and 6 °C/min and finally lyophilized (FD-10, Pishtaz Engineering Co. Iran) at temperature of -58 °C and pressure 0.5 torr for 48 hours. Unreacted glutaraldehyde removed as described in previous study (11). Briefly, the scaffolds were soaked for 1 hour in 0.1 M sodium hydroxide (NaOH), washed with deionized water (3 times) and soaked in deionized water for half an hour. Finally, all the cross-linked constructs was soaked in NaBH<sub>4</sub> 1% and then in deionized water for 2 h and 30 min; respectively, to remove unreacted glutaraldehyde. After that, scaffolds were lyophilized again.

The morphology of the scaffolds was characterized by scanning electron microscopy (SEM, Stereoscan S 360-Leica, UK) at an accelerating voltage of 20 kV. All samples were sputter-coated (Emitech K450X, Ashford, UK) with a thin layer of gold. The average diameters of resulting fibers were analyzed by image measurement software (KLONK Image Measurement Light, Edition 11.2.0.0).

Finally, the porosity of the scaffolds was calculated using Equation 1; where  $\rho_{\text{scaffold}}$  is the density of the freeze-cast structure and  $\rho_{\text{solid}}$  is the density of the bulk polymers (12).

$$\text{Porosity (\%)} = 1 - (\rho_{\text{Scaffold}} / \rho_{\text{Solid}}) * 100 \quad (1)$$

Chemical characterization of the RFC fibers were examined by the fourier transforms infrared spectrophotometer (FTIR, Nicolet Is10, USA) between 400 and 4000 cm<sup>-1</sup> with a resolution of 4.0 cm<sup>-1</sup> and 8 scans.

Mechanical properties of the scaffolds were determined by a comparison strength test system (Santam, STM 20, Iran) equipped

with a 100 N load cell under a cross-head speed of 0.5 mm/min.

The wettability of the conventional and rapid freeze casting samples was assessed by water contact angle (Kruss DSA 100, Germany) values at room temperature. The droplet size was set at 1.0 ml.

The water absorption capacity of the scaffolds was determined after immersing scaffolds in 30 ml of PBS and were incubated at 37±0.5 °C and the rotational speed of 30 rpm for 12 and 24 hours. So at each measurement time, the water on the specimen surface was removed and the specimen was weighed in wet condition. The percent of swelling is given according to the equation 2., Where W<sub>0</sub> is the initial weight and W is the wet weight of the sample.

$$\text{Swelling ratio (\%)} = [(W - W_0) / W_0] * 10 \quad (2)$$

Biodegradation rate of samples was determined using equation 3. So, the dry weight (W<sub>0</sub>) of the 3D-shaped scaffolds was measured. After that, samples were transferred into falcon tubes with 30 ml PBS and were incubated at 37±0.5 °C and the rotational speed of 30 rpm for 3, 6, 9, 12, and 15 days. At the end of each period, the PBS solution was refreshed and the samples were washed with distilled water, freeze-dried (temperature about -58 °C and pressure 0.5 torrs for 24 hours) and weighed (W) (13).

$$\text{Biodegradation ratio (\%)} = [(W - W_0) / W_0] * 100 \quad (3)$$

The biocompatibility of L929 cells on RFC fibers was investigated by MTT (3-{4,5-dimethylthiazol-2yl}-2,5-diphenyl-2Htetrazolium bromide) assay as described in our previously published work (4). The samples were sterilized by washing the bulk fibers with sterile PBS and penicillin/streptomycin (14).

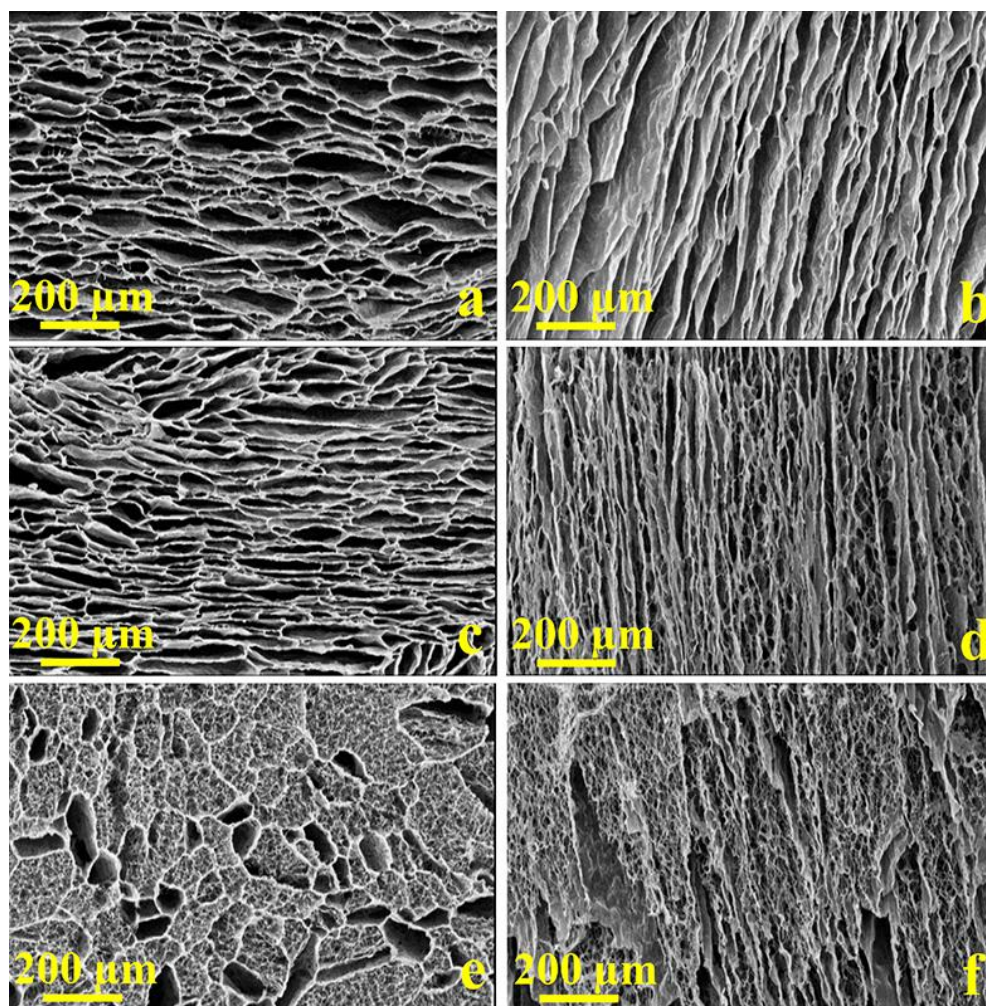


**Fig. 1:** SEM micrographs of freeze casting gelatin scaffolds (a-f) with different freezing rate (R1 (a, b), R3 (c, d), and R6 (e, f)). Figures a, c and e are perpendicular and b, d and f are parallel to the direction of solidification.

Then, they were loaded by  $5 \times 10^5$  third passage of L929 fibroblast cells supplied by Materials and Energy Research Center cell bank, Karaj, Alborz. Cell loaded samples were covered by DMEM supplemented with 15% FBS, 100 gr/ml penicillin-streptomycin and 1.2% glutamine and incubated (Incubator, MCO-19ALC, SANYO Co, Japan) in 37 °C, 5% CO<sub>2</sub> and 95% humidity for 48 hours. At each time point (3, 5, and 7 days after culturing), the medium was removed and 2 ml MTT/cell culture medium (1:5) solution was added to each well. Then,

the medium was discarded and precipitated formazan was dissolved in DMSO. The optical density of the solution was evaluated using a microplate spectrophotometer at a wavelength of 540 nm.

### 3. Results and discussion

SEM micrographs (Fig. 1(a-f)) show the lamellar morphology of CFC and RFC gelatin scaffolds. Figures indicate the ice formation in perpendicular and parallel to solidification direction and different freezing gradients from 1 to 6 °C/min.

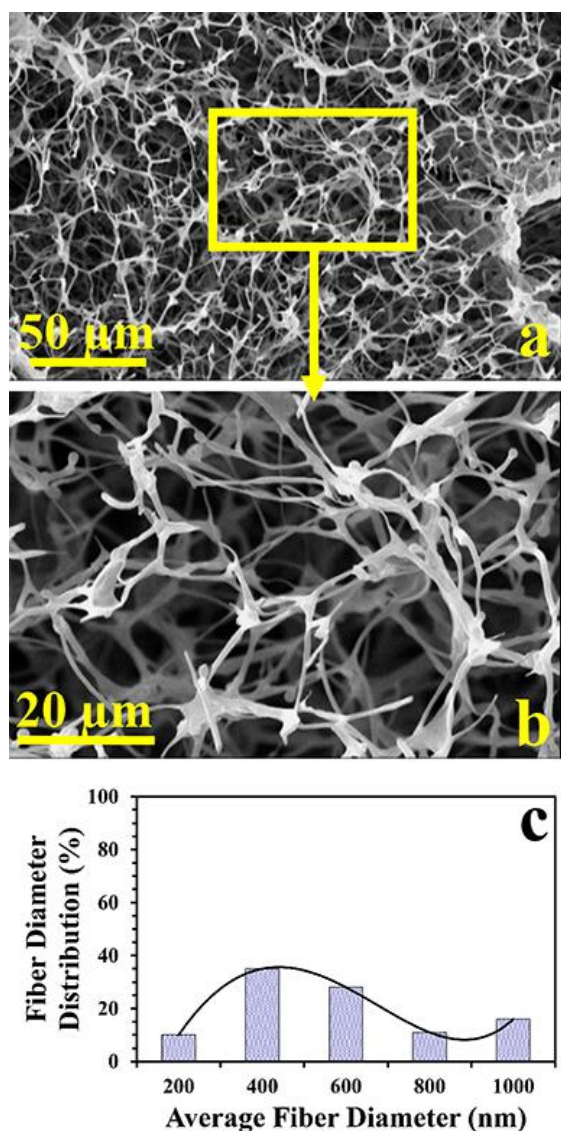


**Fig. 2:** SEM micrographs of RFC fibers (a, b) and size distribution of fibers determined by image measurement software (c).

Freeze casting scaffolds represent interconnected lamellar type microstructure (15) with approximately 98% porosity according to Eq.1, whereas elongated pores were generated in the direction of ice nucleation and growth. Accordingly, applying a temperature gradient in a certain direction and increasing heat transfer reduces pore diameter, as other investigations (11,16).

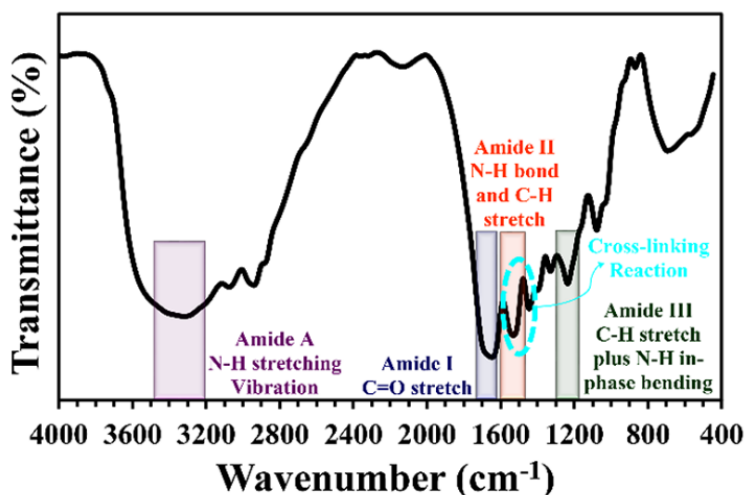


**Fig. 3:** FTIR spectrum of cross-linked RFC fibers.

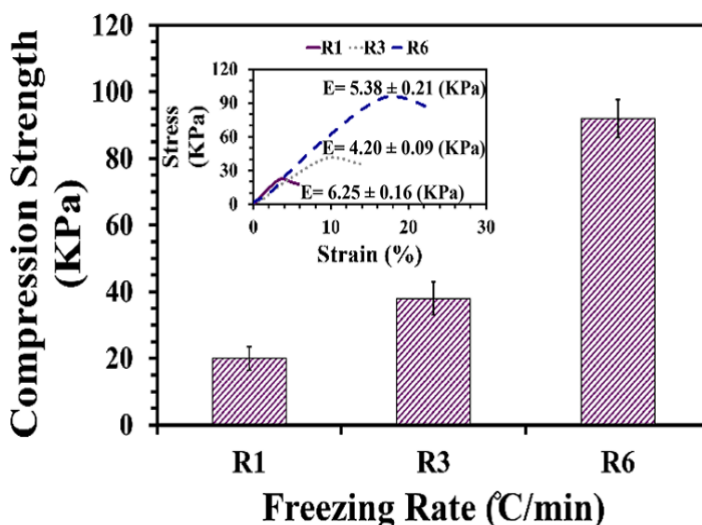


**Fig. 4:** Compression strength and stress-strain curves of both CFC and RFC scaffolds.

Obtained results demonstrate that in higher solidification rate porous scaffolds alter to bulky and narrow fibers (Fig. 1(e-f) and Fig. 2(a, b)) with diameter in the range of 200-1000 nm (Fig. 2c). RFC 3D-shaped nanofibers with smooth surface can be fabricated from all single or blend materials at different applied freezing gradients.

This technique provides an opportunity to change the diameter of the fibers by controlling the solidification rate via nitrogen charging and PID (proportional–integral–derivative) controller of freezing set up. It is expected that increasing the freezing rate leads to the formation of thinner fibers. Novel RFC technique compensates problems of mass production and mat or film-like fibers that observed in other methods.

Fig. 3 shows FTIR spectra of cross-linked gelatin fibers. Vibration peaks at  $1636\text{ cm}^{-1}$  and  $1528\text{ cm}^{-1}$  can be related to amide I band and II in gelatin, respectively. C-H stretch plus N-H bending vibration at  $1260\text{ cm}^{-1}$  and

N-H stretching vibration at  $3320\text{ cm}^{-1}$  attributes to Amide III and Amide A, respectively. Additional peaks observed at  $1470\text{--}1570\text{ cm}^{-1}$  corresponds to cross-linking reactions by glutaraldehyde to improve stability. Fortified scaffolds can tolerate stresses during regeneration. Created unidirectional pores in freeze casting technique greatly enhanced mechanical properties as Deville observation (17). Compression strength and stress-strain curves of gelatin scaffolds (Fig. 4) confirmed the improvement of mechanical strength and toughness by increasing temperature gradient.

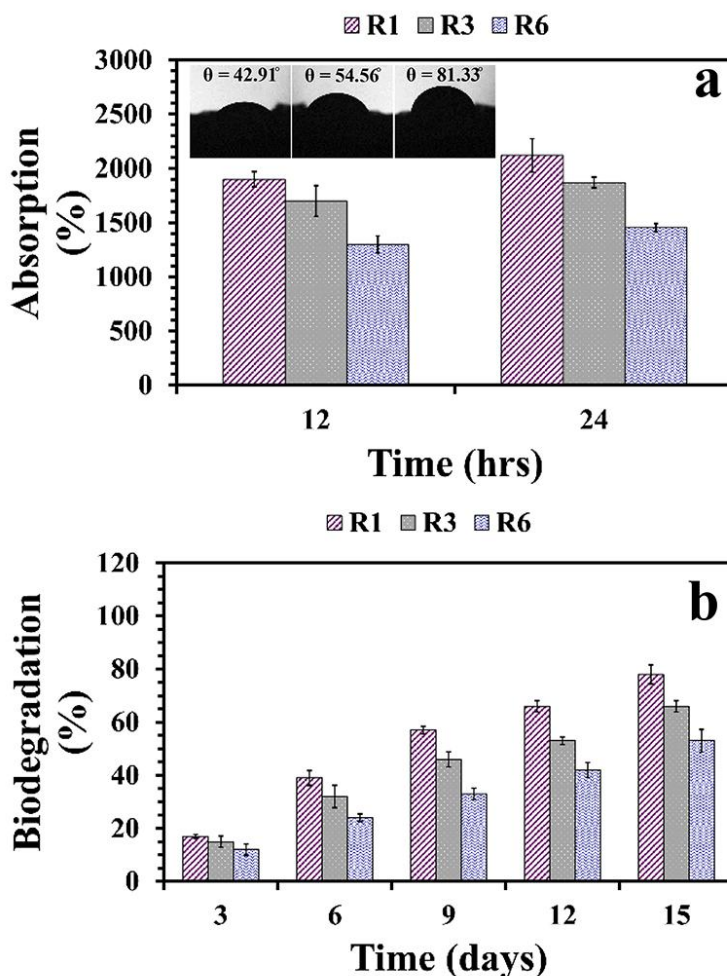


**Fig. 5:** A 12-hour and 24-hour PBS absorption capacity and hydrophilicity measurements of scaffolds (a) and biodegradation rate of CFC scaffolds and RFC fibers. (Differences between all the groups in a compression test, R1-R6 and R3-R6 in swelling ratio analysis after 12 and 24 hours, respectively, and R1-R6 in biodegradation test after 9 weeks is statistically significant.)

Hence, the compressive strength was found to depend on the solidification rate. Producing smaller pores cause a significant number of walls along unidirectional channels that withstands and transfers applied stresses. Accordingly, 3D-shaped nanofibrous scaffolds gain the highest strength compared with porous structures. So, RFC is the promising method provides production of durable nanofibers in the very low concentration of polymer solution. Although another study (18) indicated that addition of gelatin to polymeric scaffolds induces brittle nature with low stiffness, RFC technique produced gelatin fibers with adequate compression strength. The absorption capacity of the fibers affects the healing process by controlling cellular mechanisms. Swelling ratio and hydrophilicity of CFC and RFC samples (Fig. 5a) determined that unidirectional pores in freeze casting operation resulted in high

values of absorption such as similar investigation (10). Accordingly, increasing heat transfer decreased PBS absorption because of pore size reduction and difficulties in fluid diffusion; however, RFC fibers allocates a permissible range of swelling to itself compared with other fiber production techniques (19). Increasing the water drop contact angle as a function of freezing rate enhancement confirmed all the above achievements. Small pores in R6 freezing gradient led to improvement of mechanical strength and resistance to absorption fluids; therefore, the RFC scaffolds keep their stability during 15-day experiment and degraded slowly (Fig. 5b) compared with CFC scaffolds. Changing the solidification rate provides this opportunity to fabricate desired fiber diameter with controllable biodegradable behavior based on our needs.

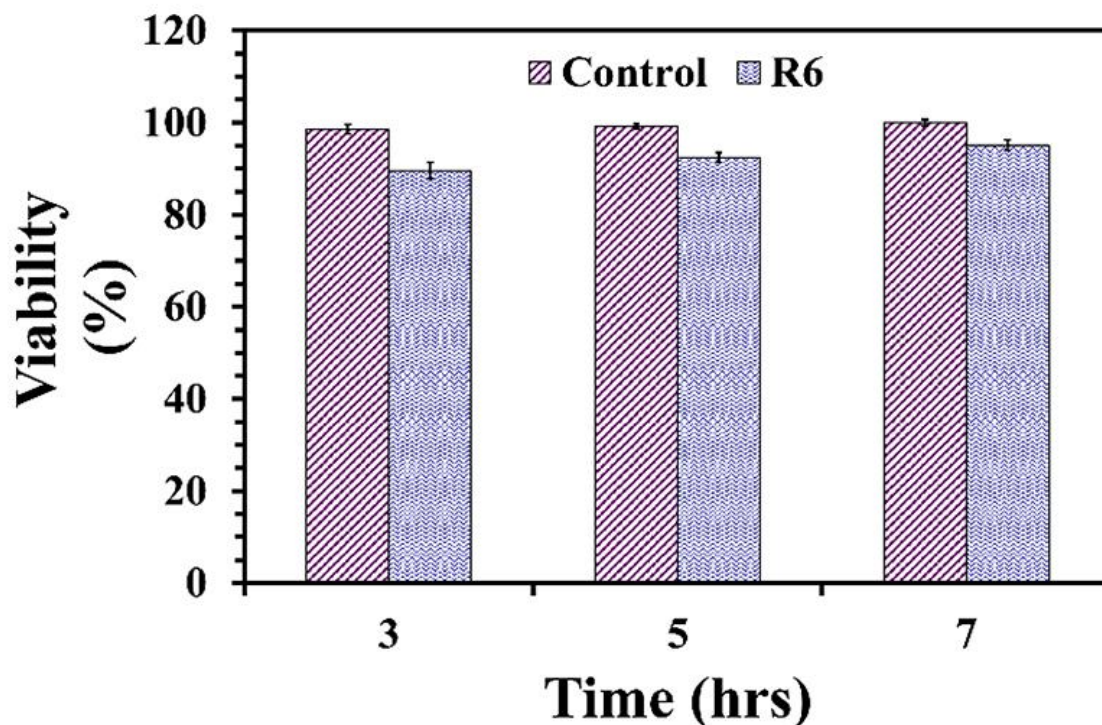


**Fig. 6:** The cellular viability of gelatin RFC fibers after a 3-day, 5-day, and 7-day L929 fibroblast cells culture. Seeded cells on a plate served as a control group.

The viability of cultured cells on RFC fibers (Fig. 6) illustrates fibers are biocompatible and support cellular proliferation. Enhancing the number of viable cells till 7th days could be owing to ameliorated cellular transfer and reduction of cell stresses. However, the viability of more than 90% cells proves that polymeric fibers have the initial biological feature for further biological studies.

#### 4. Conclusion

A novel technique, RFC, was studied for fabricating 3D-shaped nanofibers. CFC and RFC prepared-scaffolds showed unidirectional microstructure, while porous scaffolds alter fibers with 3D macrostructure by increasing solidification rate. The capability of bulk production with significant strength instead of mat or film-like fibers is the power of this study. The ability to control fiber diameter and biodegradation rate of RFC fibers by changing freezing gradient has made this method acceptable for further in-vitro and in-vivo studies in tissue engineering field.

#### References

1. Sangkert S, Kamonmattayakul S, Chai WL, Meesane J. A biofunctional-modified silk fibroin scaffold with mimic reconstructed extracellular matrix of decellularized pulp/collagen/fibronectin for bone tissue engineering in alveolar bone resorption. *Mater Lett* [Internet]. 2016 Mar;166:30–4. Available from: <http://linkinghub.elsevier.com/retrieve/pii/S0167577X15309824>.
2. Boccaccini AR, Ma PX. Tissue engineering using ceramics and polymers. 2014.
3. Unnithan AR, Arathyram RS, Kim CS. Electrospinning of polymers for tissue engineering [Internet]. *Nanotechnology Applications for Tissue Engineering*. Elsevier Inc.; 2015. 45-55 p. Available from: <http://linkinghub.elsevier.com/retrieve/pii/B978032332889000030>
4. Ghorbani F, Nojehdehyan H, Zamanian A, Gholipourmalekabadi M, Mozafari M. Synthesis, physico-chemical characteristics and cellular behavior of poly (lactic-co-glycolic acid)/gelatin nanofibrous scaffolds for engineering soft connective tissues. *Adv Mater Lett*. 2016;7(2):163–9.
5. Mi HY, Jing X, Yu E, McNulty J, Peng XF, Turng LS. Fabrication of triple-layered vascular scaffolds by combining electrospinning, braiding, and thermally induced phase separation. *Mater Lett* [Internet]. 2015;161:305–8. Available from: <http://dx.doi.org/10.1016/j.matlet.2015.08.119>
6. Ariga K, Hill JP, Lee M V, Vinu A, Charvet R, Acharya S. Challenges and breakthroughs in recent research on self-assembly. *Sci Technol Adv Mater*. 2008;9(1):14109.
7. Vinogradov G V., Yarlykov B V., Tsebrenko M V., Yudin A V., Ablazova TI. Fibrillation in the flow of polyoxymethylene melts. *Polymer (Guildf)*. 1975;16(8):609–14.
8. Ndaro MS, Xiangyu J, Ting C, Yu C. Effect of impact force on tensile properties and fiber splitting of splittable bicomponent hydroentangled fabrics. *Fibers Polym*. 2007;8(4):421–6.
9. Benavides RE, Jana SC, Reneker DH. Nanofibers from Scalable Gas Jet Process. *ACS Macro Lett* [Internet]. 2012 Aug 21;1(8):1032–6. Available from: <http://pubs.acs.org/doi/abs/10.1021/mz300297g>
10. Ghorbani F, Zamanian A, Nojehdehian H. Effects of pore orientation on in-vitro properties of retinoic acid-loaded PLGA/gelatin scaffolds for artificial peripheral nerve application. *Mater Sci Eng C* [Internet]. 2017 Mar;77:159–72. Available from: <http://linkinghub.elsevier.com/retrieve/pii/S0928493116321634>
11. Ghorbani F, Nojehdehian H, Zamanian A. Physicochemical and mechanical properties of freeze cast hydroxyapatite-gelatin scaffolds with dexamethasone loaded PLGA microspheres for hard tissue engineering applications. *Mater Sci Eng C* [Internet]. 2016 Dec;69:208–20. Available from: <http://linkinghub.elsevier.com/retrieve/pii/S092849311630649X>
12. Salgado AJ, Gomes ME, Chou A, Coutinho OP, Reis RL, Huttmacher DW. Preliminary study on the adhesion and proliferation of human osteoblasts on starch-based scaffolds.



- Mater Sci Eng C [Internet]. 2002 May;20(1–2):27–33. Available from: <http://www.sciencedirect.com/science/article/pii/S0928493102000097>
13. Wu X, Liu Y, Li X, Wen P, Zhang Y, Long Y, et al. Preparation of aligned porous gelatin scaffolds by unidirectional freeze-drying method. *Acta Biomater* [Internet]. 2010 Mar [cited 2013 Nov 24];6(3):1167–77. Available from: <http://www.ncbi.nlm.nih.gov/pubmed/19733699>
  14. Cai J, Ziemba KS, Smith GM, Jin Y. Evaluation of cellular organization and axonal regeneration through linear PLA foam implants in acute and chronic spinal cord injury. *J Biomed Mater Res Part A* [Internet]. 2007 Nov;83A(2):512–20. Available from: <http://doi.wiley.com/10.1002/jbm.a.31296>
  15. Zamanian A, Farhangdoust S, Yasaei M, Khorami M, Hafezi M. The effect of particle size on the mechanical and microstructural properties of freeze-casted macroporous hydroxyapatite scaffolds. *Int J Appl Ceram Technol* [Internet]. 2014 Jan 4;11(1):12–21. Available from: <http://doi.wiley.com/10.1111/ijac.12031>
  16. Farhangdoust S, Zamanian A, Yasaei M, Khorami M. The effect of processing parameters and solid concentration on the mechanical and microstructural properties of freeze-casted macroporous hydroxyapatite scaffolds. *Mater Sci Eng C Mater Biol Appl* [Internet]. 2013 Jan 1 [cited 2015 Apr 25];33(1):453–60. Available from: <http://www.ncbi.nlm.nih.gov/pubmed/25428095>
  17. Deville S. *Freezing Colloids: Observations, Principles, Control, and Use* [Internet]. Cham: Springer International Publishing; 2017. (Engineering Materials and Processes). Available from: <http://link.springer.com/10.1007/978-3-319-50515-2>
  18. Li X-K, Cai S-X, Liu B, Xu Z-L, Dai X-Z, Ma K-W, et al. Characteristics of PLGA-gelatin complex as potential artificial nerve scaffold. *Colloids Surf B Biointerfaces* [Internet]. 2007 Jun 15 [cited 2015 Oct 11];57(2):198–203. Available from: <http://www.ncbi.nlm.nih.gov/pubmed/17368867>
  19. Zhang S, Huang Y, Yang X, Mei F, Ma Q, Chen G, et al. Gelatin nanofibrous membrane fabricated by electrospinning of aqueous gelatin solution for guided tissue regeneration. *J Biomed Mater Res A*. 2009;90:671–9.